

Specific heat of single crystal MgB_2 : a two-band superconductor with two different anisotropies

F. Bouquet,¹ Y. Wang,¹ I. Sheikin,¹ T. Plackowski,¹ A. Junod,¹ S. Lee,² and S. Tajima²

¹*DPMC, University of Geneva, 24 quai Ernest-Ansermet, 1211 Genève 4, Switzerland*

²*Superconductivity Research Laboratory, ISTEC, 1-10-13 Shinonome, Koto-ku, Tokyo 135-0062, Japan*

(Dated: August 23, 2019)

Heat-capacity measurements of a 39 μg MgB_2 single crystal in fields up to 14 T and below 3 K allow the determination of the low-temperature linear term of the specific heat, its field dependence and its anisotropy. Our results are compatible with two-band superconductivity, the band carrying the small gap being isotropic, that carrying the large gap having an anisotropy of ~ 5 . Three different upper critical fields are thus needed to describe the superconducting state of MgB_2 .

PACS numbers: 74.70.Ad, 74.25.Bt, 74.60.Ec, 74.25.Jb.

Shortly after the discovery of 40-K superconductivity in MgB_2 [1], its nature was intensively studied. The isotopic effect soon indicated phonon-mediated pairing [2]. However, MgB_2 cannot be considered as a classic conventional superconductor; indeed several studies point to the existence of a gap much smaller than the expected BCS value: band-structure calculations [3, 4], STM [5, 6], specific heat (C) [7, 8, 9, 10, 11], penetration depth [12], and various spectroscopic experiments [13, 14, 15, 16, 17]. The so-called “two-band” model [3, 4], which considers two different superconducting gaps on separate sheets of the Fermi surface, now seems widely accepted and explains most experimental results [18, 19], with few exceptions [20]. The theory of two-band superconductivity was suggested soon after the outcome of the BCS theory [21], and some s-d metals have shown hints of this phenomenon, generally in the form of small deviations from BCS predictions, e.g. in C experiments [22]. In contrast, MgB_2 shows so clear signatures that it might serve as a textbook example. For instance, the electronic specific heat of MgB_2 shows an excess by an order of magnitude at $\sim T_c/5$, and presents an exponential dependence at low temperature (T) indicating the existence of a small gap on a large fraction ($\sim 50\%$) of the Fermi surface [7, 8, 9, 10, 11]. At low T the effect of a small magnetic field (H) on the coefficient of the linear C -term (γ) is dramatic. In a simple one-band, s-wave model, $\gamma(H)$ should be linear up to H_{c2} . Generally speaking, anisotropy may cause deviations, but for MgB_2 an extreme non-linearity was observed, which was related to the existence of an additional, smaller gap [7, 8, 9, 10].

The only specific heat experiment on single crystal reported so far was focused on the superconducting transition [23, 24]. Such experiments are delicate since the mass of MgB_2 crystals is usually smaller than 100 μg , but are required to study the anisotropy. Previous studies showed that the anisotropy of superconducting properties depends on both field and temperature [25, 26]. This puzzling behavior motivated the present study.

We present a study of the low-temperature specific heat of a MgB_2 single crystal with the field parallel and perpendicular to the boron planes. The results clearly

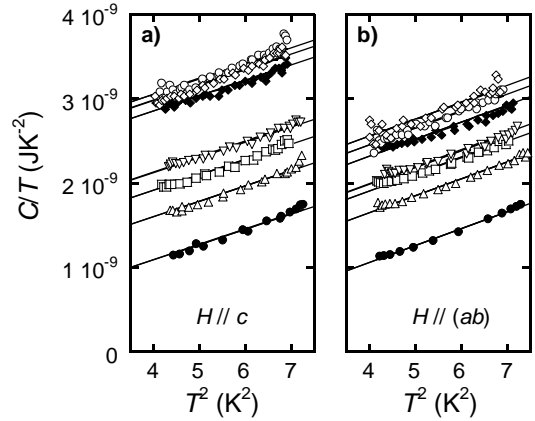


FIG. 1: Typical curves of total specific heat, including that of addenda, for different magnetic fields (\bullet : 0 T; \triangle : 0.2 T; \square : 0.5 T; ∇ : 1 T; \blacklozenge : 3 T; \circ : 6 T; \diamond : 10 T) applied; **a**) along the c -axis; **b**) in the (ab) -planes.

show that the extreme non-linearity of $\gamma(H)$ is an intrinsic property of MgB_2 , related to the existence of two superconducting gaps, rather than to the polycrystalline nature of previous samples [7, 8, 9, 10]. Moreover, these measurements reveal a dramatic variation of the effective anisotropy with the field, from 1 to ~ 5 . We interpret these results as a manifestation of the two-band nature of the superconductivity of MgB_2 , one band being isotropic (and carrying the smaller gap), the other one being anisotropic (and carrying the larger gap).

The single crystal of MgB_2 is similar to those described in Ref. [27]. Its mass, 39 μg , is small for a quantitative study of specific heat. For this purpose, we developed a miniaturized version of the relaxation calorimeter used in Ref. [7]. A commercial Cernox bare chip [28] was thinned down to 1 mg mass and used at the same time as a sample platform, heater and thermometer. Two 10 μm phosphor-bronze wires soldered onto the chip were acting as mechanical support, thermal link and electrical contact. Only low- T studies were possible, since the heat capacity of the platform, essentially of phononic origin (sapphire), increases rapidly with T . We thus restrained

our study to the range 2 to 3 K. Owing to the small value of C at these temperatures, the relaxation time was short (0.1–0.5 s), necessitating aperture times shorter than one power line cycle for the digitalization of voltages. In order to suppress the 50 Hz noise, the signal was averaged over 50 to 200 relaxations. The field dependence of the addenda represents at most 13% of the normal electronic linear term of the MgB_2 crystal, and was calibrated by measuring a 196 μg Ag reference sample.

Figure 1 shows the specific heat for both orientations. It is impossible to compensate exactly for the small but unknown quantity of GE-varnish used to glue the sample. Instead, in order to calculate $\gamma(H)$, we used the zero-field curve as a reference. It was shown on polycrystals that the electronic specific heat of MgB_2 is negligible in zero field in this temperature range [8, 9, 10]. Subtracting the zero-field curves eliminates the addenda and phonon contributions, leaving that of electrons alone.

We fitted the total specific heat by a linear electronic term $\gamma(H)T$ plus a T^3 lattice term, imposing the same Debye temperature for all fields: the curves C/T vs. T^2 are parallel, but move upward with the field, indicating the presence of normal carriers at low T . The shift of the linear term gives the variation of γ with H , which is plotted in Fig. 2 for both orientations. With the field perpendicular to the boron planes, $\gamma(H)$ saturates above 4 T, indicating that the sample has entered the normal state. This value is consistent with previous reports giving $\mu_0 H_{c2}^{(c)} \approx 3$ T for the upper critical field along the c -axis [23, 24, 25, 29]. This also determines the normal electronic linear term $\gamma_n = 0.76 \pm 0.03 \text{ mJ gat}^{-1} \text{ K}^{-2}$, comparable with literature values [7, 8, 9, 10]. The normal state is not fully reached when the field is parallel to the (ab) -planes, indicating that $H_{c2}^{(ab)}$ is higher than the maximum applied field of 14 T. An extrapolation suggests $\mu_0 H_{c2}^{(ab)} \approx 18\text{--}22$ T, in general agreement with reported values [30]. Therefore, the anisotropy of the upper critical field at low temperature is established in bulk.

The anisotropy of MgB_2 has long been debated [30]. With the availability of single crystals, the values of $H_{c2}^{(c)}$ and $H_{c2}^{(ab)}$ were confirmed by several experiments using clean samples [23, 24, 25, 26, 29]. Two kinds of anisotropy can be considered: the anisotropy of the superconducting gap, and that of the Fermi surface. To model the former, some \vec{k} -dependence of the gap has to be assumed. Such an approach was attempted using a one-band model for MgB_2 [31]. Although a detailed agreement with experiment was not obtained, prominent features were qualitatively reproduced. The two-band model is an extreme case of such an anisotropy: depending on which Fermi sheet is considered, the superconducting gap may be either large or small. The effect of an anisotropic Fermi surface on superconducting properties can be modeled by renormalizing the isotropic results by a function of the ratio of the effective masses, a method that was successfully applied to the cuprate su-

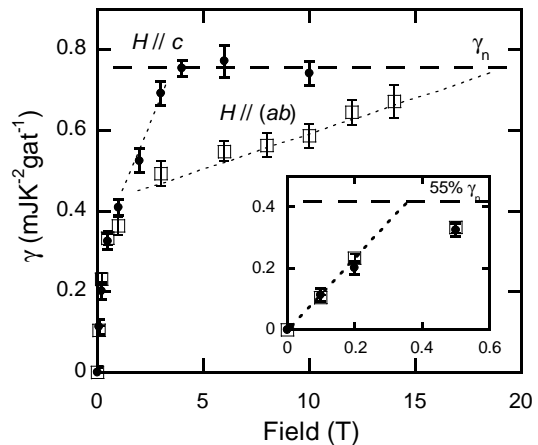


FIG. 2: Coefficient of the electronic linear term versus magnetic field applied parallel (\square) or perpendicular (\bullet) to the boron planes. The long-dashed line represents the normal state contribution. The short-dashed lines are guides for the eyes. Inset: expanded view of the low-field region; here the long-dashed line represents the partial normal-state contribution of the small-gapped band (see text and Fig. 4).

perconductors [32]. Angst *et al.* used this approach for MgB_2 [25]; however, they showed that the shape of the torque curves did not follow this model over the whole range of field orientations.

From Fig. 2, it is clear that it is not possible to normalize the effect of the field over the whole range using a constant factor. At low H , the values of $\gamma(H)$ are almost undistinguishable, irrespective of the field direction, showing the absence of anisotropy below 0.5 T (see inset of Fig. 2). However, a value of ~ 5 is needed to scale the $\gamma(H)$ curves near the upper critical fields. An effective anisotropy Γ_{eff} can be defined as the scaling factor by which the field along the c -axis must be multiplied in order to merge both $\gamma(H)$ curves. Figure 3 presents Γ_{eff} versus $H/(ab)$. At low field, $\Gamma_{eff} \approx 1$, since the effect of H does not measurably depend on the orientation; Γ_{eff} rapidly increases with H , and tends toward the anisotropy of H_{c2} , ~ 5 . Such an H -dependent anisotropy was also deduced from torque measurements [25]. The present analysis shows that the change of Γ_{eff} with H (and possibly with T) is an intrinsic property of MgB_2 , having a bulk thermodynamic signature, even though the amplitude of this variation may depend on the physical quantity by which it is determined. We will argue in the following that, to explain specific heat measurements, both kinds of anisotropies are required: that of the two-gap model *plus* a renormalization by the effective masses on the relevant Fermi sheets.

Let us first focus on the shape of the $\gamma(H)$ curves. Similarly to previous data on polycrystals, $\gamma(H)$ increases sharply at low fields. The present data show that this effect is intrinsic and does not depend on the orientation of the field. This increase demonstrates the existence of a large fraction of normal electrons in the mixed state

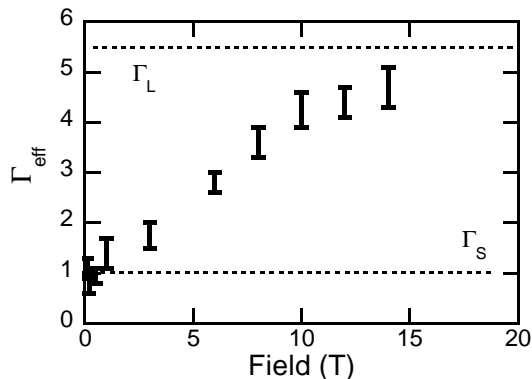


FIG. 3: Effective anisotropy, defined as the ratio of magnetic fields applied in the (ab) -planes and along the c -axis yielding the same γ -value. Note that the choice of the abscissa is arbitrary: we chose $H// (ab)$, but we could as well plot it versus $H//c$ or versus $\gamma(H)$.

at low H . In a typical s -wave type-II superconductor, this contribution mainly comes from the vortex cores and should be approximatively proportional to the magnetic field (that is, the number of vortices). The strong non-linearity of $\gamma(H)$ for MgB_2 is atypical: for $\mu_0 H = 1$ T, approximatively half of γ_n is recovered, irrespective of the field direction. The effect is particularly striking for $H// (ab)$: about 5% of $H_{c2}^{(ab)}$ drives $\sim 50\%$ of the electrons into the normal state.

The peculiar shape of $\gamma(H)$ can be understood by considering the meaning of a vortex within a two-band model. Both bands supply the carriers and currents that define one vortex, and both bands contribute to the local density-of-states (LDOS) in one vortex core. Simulations [33] and STM studies [6] suggest that a core results from the superposition of two peaks in the LDOS with different diameters, defined as usual by the coherence length ξ_L or ξ_S associated with each band. The peaks with diameter ξ_L lead to a conventional core contribution for the L-band, and overlap at H_{c2} . In contrast, the large coherence length of the S-band gives rise to broader LDOS peaks, in the sense that their diameter is much larger than $(\Phi_0/2\pi H_{c2})^{1/2}$. The resulting giant cores, which have been observed by STM [6], contribute heavily to the total low-T DOS, as measured by $\gamma(H)$, until they start to overlap much below H_{c2} . At this point, the contribution of the S-band to $\gamma(H)$ saturates. At higher fields, superconductivity in the S-band is maintained up to H_{c2} by coupling with the L-band, but the variation of $\gamma(H)$ comes from the L-band contribution. The $\gamma(H)$ curves of Fig. 2 compare qualitatively well with the predictions of Ref. [33] (the analysis of the results of previous measurements on polycrystalline samples [7, 8, 9, 10] was complicated by angular averaging of $\gamma(H//c)$ and $\gamma(H//ab)$, leading to a flattening above 8 T).

In the present scheme, the data of Fig. 2 can be used to determine the anisotropy of each contribution (resp.

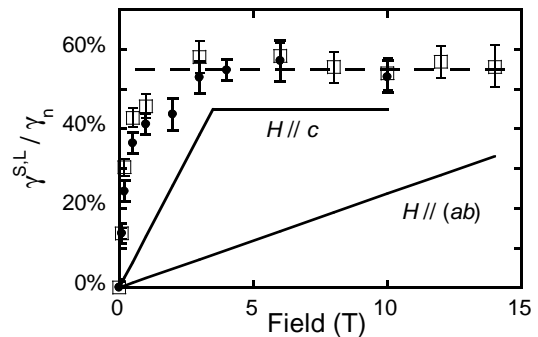


FIG. 4: Separation of the contributions to $\gamma(H)$ of the S-band (data points) and the L-band (calculated straight lines, see text) for the field applied along the c -axis (\bullet) and in the (ab) -planes (\square). The dashed line represents to the normal contribution of the S-band (55% of γ_n).

Γ_S and Γ_L). The contribution of the S-band does not depend on the field orientation, therefore $\Gamma_S \approx 1$. On the other hand, the L-band contribution is responsible for the anisotropy of H_{c2} , therefore $\Gamma_L \approx 5$. Indeed, band-structure calculations attribute a 3D nature to the S-band, whereas the L-band should be rather 2D. The *effective* anisotropy shown in Fig. 3 is a weighted average which depends on contributions of each band to the condensate for given H and T : it tends toward Γ_S at low fields, and toward Γ_L at high fields.

Both contributions can be further separated using a simple model. We postulate that the contribution of the L-band follows a typical s -wave behavior, i.e. a linear increase from $\gamma(0) = 0$ to $\gamma(H_{c2}) = \gamma_n$, with an anisotropic H_{c2} . This contribution is subtracted from the measured $\gamma(H)$ to obtain the S-band contribution. There are three free parameters in this procedure: $H_{c2}^{(c)}$, $H_{c2}^{(ab)}$, and the ratio between the contributions of both bands to γ_n . Figure 4 shows the result, with $\mu_0 H_{c2}^{(c)} = 3.5$ T, $\mu_0 H_{c2}^{(ab)} = 19$ T, and a ratio of 55:45 for the S:L contributions. This set of parameters is not unique, but it is difficult to get reasonable fits with values differing by more than 15%. The H_{c2} anisotropy, associated with the L-band, is $\Gamma_L \approx 5.5$, close to the low- T value 6 reported in Ref. [25] (Γ_L and Γ_S are represented by dashed lines in Fig. 3). Another important parameter is the S:L ratio, close to 1:1. This result, obtained from field-dependent data, is consistent with zero-field fits of specific-heat [11], penetration-depth [12] experiments, and band-structure calculations [4, 18, 19]. Figure 4 shows that the obtained S-band contribution appears to be isotropic over the whole range of fields, and follows quantitatively the calculation of Nakai *et al.* [33] or the simulation made by Eskildsen *et al.* [6]. This shows that a model considering two superfluids of equal weighing, each with a different superconducting gap and a different anisotropy, gives a consistent description of various properties for MgB_2 .

The recent measurements of the thermal conductivity of single crystals by Sologubenko *et al.* [29] may be

interpreted in a similar way. At low fields, the heat conductivity increases sharply, for all field directions. As discussed for $\gamma(H)$, this is attributed to the contribution of normal 3D S-band carriers in the anomalously large vortex cores. At higher field, this effect saturates and the anisotropy rises, due to the increasing contribution of the quasi 2D L-band. A similar approach may explain not only why the anisotropy obtained from magnetic torque experiment changes with field and temperature, but also why a single-anisotropy model does not fit the angular dependence of H_{c2} [25, 26]. We emphasize, however, that this view is simplified and phenomenological. A more elaborate description for the interaction between the two bands was proposed [34, 35] for the anisotropy of penetration depth and its temperature dependence (which can be understood as a consequence of the rapid thermal depletion of the isotropic S-band condensate).

The phenomenological two-band model of Ref. [11] also uses two independent superfluids to explain the zero-field C of MgB_2 . Inter-band coupling was introduced by considering that the “virtual” T_c of the S-band ($\Delta_S/1.76k_B \sim 10$ K) is brought up to that of the L-band; the peculiar features in C then originate from this superconductivity “above T_c ”. Here a somewhat similar situation arises: a “virtual” upper critical field can be defined for the S-band, $H_{c2}^S = (\Phi_0 \pi^2 \Delta_S^2) / (2\pi \hbar^2 v_F^2)$; superconductivity persists up to $H_{c2}^{(c)}$ or $H_{c2}^{(ab)}$, depend-

ing on the field orientation, but above H_{c2}^S the overlap of huge vortex cores drives the majority of the S-band electrons normal (superconductivity “above H_{c2} ”). Three characteristic fields are thus needed to describe the physics of MgB_2 : the two upper-critical fields $H_{c2}^{(c)}$ and $H_{c2}^{(ab)}$ associated with the anisotropic L-band, and a cross-over field H_{c2}^S associated with the S-band. We estimate the latter one by linearly extrapolating the low field $\gamma(H)$ to the partial normal-state γ for this band ($\sim 0.55\gamma_n$), by analogy with classic superconductors. The inset of Fig. 2 shows this construction: we find $\mu_0 H_{c2}^S \approx 0.3\text{--}0.4$ T. This fields determine the values of the three coherence lengths of the system: for the anisotropic L-band $\xi_L^{(ab)} \sim 10$ nm and $\xi_L^{(c)} \sim 2$ nm; for the isotropic S-band $\xi_S \sim 30$ nm. The latter value compares favorably with a direct measurement by STM giving 50 nm for the vortex-core diameter in the S-band [6]. All *three* fields are needed to give a phenomenological description of the superconducting properties of MgB_2 .

Stimulating discussions with M. R. Eskildsen, T. Dahm, C. Berthod, and C. Marcenat are gratefully acknowledged. This work was supported by the Swiss National Science Foundation through the National Centre of Competence in Research “Materials with Novel Electronic Properties-MaNEP” and the New Energy and Industrial Technology Development Organization (NEDO).

-
- [1] J. Nagamatsu *et al.*, Nature **410**, 63 (2001).
 - [2] S. L. Bud’ko *et al.*, Phys. Rev. Lett. **86**, 1877 (2001).
 - [3] S. V. Shulga *et al.*, cond-mat/0103154.
 - [4] A. Y. Liu, I. I. Mazin, and J. Kortus, Phys. Rev. Lett. **87**, 087005 (2001).
 - [5] G. Rubio-Bollinger, H. Suderow, and S. Vieira, Phys. Rev. Lett. **86**, 5582 (2001).
 - [6] M. Eskildsen *et al.*, submitted to PRL.
 - [7] Y. Wang *et al.*, Physica C **355**, 179 (2001).
 - [8] F. Bouquet *et al.*, Phys. Rev. Lett. **87**, 047001 (2001).
 - [9] A. Junod *et al.*, *Studies of High Temperature Superconductors* (Nova Publishers, Commack (N.Y.) ed. Narlikar) **38**, 179 (2002).
 - [10] H. D. Yang *et al.*, Phys. Rev. Lett. **87**, 167003 (2001).
 - [11] F. Bouquet *et al.*, Europhys. Lett. **56**, 856 (2001).
 - [12] F. Manzano *et al.*, Phys. Rev. Lett. **88**, 047002 (2002).
 - [13] X. K. Chen *et al.*, Phys. Rev. Lett. **87**, 157002 (2001).
 - [14] S. Tsuda *et al.*, Phys. Rev. Lett. **87**, 177006 (2001).
 - [15] F. Giubileo *et al.*, Phys. Rev. Lett. **87**, 177008 (2001).
 - [16] P. Szabó *et al.*, Phys. Rev. Lett. **87**, 137005 (2001).
 - [17] F. Laube *et al.*, Europhys. Lett. **56**, 296 (2001).
 - [18] A. A. Golubov *et al.*, J. Phys.: Condens. Matter **14**, 1353 (2002).
 - [19] H. J. Choi *et al.*, cond-mat/0111183.
 - [20] H. Kotegawa *et al.*, cond-mat/0201578.
 - [21] H. Suhl, B. T. Matthias, and L. R. Walker, Phys. Rev. Lett. **3**, 552 (1959).
 - [22] L. Y. L. Shen, N. M. Senozan, and N. E. Phillips, Phys. Rev. Lett. **14**, 1025 (1965).
 - [23] U. Welp *et al.*, cond-mat/0203337.
 - [24] L. Lyard *et al.*, cond-mat/0206231.
 - [25] M. Angst *et al.*, Phys. Rev. Lett. **68**, 167004 (2002).
 - [26] Y. Eltsev *et al.*, cond-mat/0202133.
 - [27] S. Lee *et al.*, J. Phys. Soc. Jap. **70**, 2255 (2001).
 - [28] CX-1050-BR, see www.lakeshore.com.
 - [29] A. V. Sologubenko *et al.*, Phys. Rev. B **66**, 014504 (2002).
 - [30] C. Buzea, and T. Yamashita, Superconductors Science & Technology **14**, R115 (2001).
 - [31] A. I. Posazhennikova, T. Dahm, and K. Maki, cond-mat/0204272.
 - [32] G. Blatter *et al.*, Rev. Mod. Phys. **66**, 1125 (1994).
 - [33] N. Nakai, I. Masanori, and K. Mashida, J. Phys. Soc. Jap. **71**, 23 (2002).
 - [34] V. G. Kogan, cond-mat/0204038.
 - [35] A. A. Golubov *et al.*, cond-mat/0205154.